

Dynamic evolution of near-UV emission spectrum observed in the microwave plasma-surface interaction

A. Matsubara¹, S. Takayama², K. Nakayama¹, T. Kanaba¹, M. Tomimoto¹, R. Akiyama², S. Okajima¹, and M. Sato²

¹Chubu University, 1200, Matsumoto, Kasugai, Aichi, 487-8501, Japan

²National Institute for Fusion Science, 322-6 Oroshi, Toki, Gifu, 509-5292, Japan

The material heating during the carbothermic reduction of magnetite in a 2.45 GHz microwave multimode furnace has been investigated with multipoint spectroscopic measurements. The heating mode shifts from volumetric heating to plasma heating after sudden rise in temperature of the material from ~700 °C to ~1000 °C accompanied by the light emission of plasma. Then, the emission spectrum in the near-UV range (240 nm - 310 nm) changes drastically from a continuous spectrum to a discrete line spectrum with increasing temperature of material, representing progress of reduction process of iron oxide. The position dependency of the spectral evolution indicates the importance of the plasma-surface interaction in the large-scale surface structure on the material.

Keywords: plasma surface interaction, microwave iron making, reduction process, spectroscopy, near-UV emission, continuous spectrum, cathodoluminescence, surface structure.

1. Introduction

Plasma-surface interaction that is one of crucial issues in fusion research as well as plasma processing has been studied in some cases in field of the microwave material processing also. The microwave processing is based on the heating of material under the microwave irradiation. The microwave energy absorbed into the material transfers consequently to the thermal energy of the material. The main advantage of that method enables volumetric heating of materials since the absorption length is comparable or larger than the scale length of most electrically insulating materials such as ceramics, polymers, and certain composite materials, even metal if it is powdered state, as a rule, leading significant energy savings and reduction in process time. Sometimes electric discharge occurs on the surface of the material, which has been believed to be helped by the presence of vapours of various substances and thermal electrons emerging from hot spots on the surface. The occurrence of the discharge has been routinely to be avoided, because the volumetric heating is lost; the part of microwave energy is absorbed as the kinetic energy of the plasma electron. However a few applications utilize such plasma in order to modify the surface condition or boost specific chemical reaction. One of the applications is microwave ironmaking presented here.

High-purity pig irons have been produced successfully in a multimode microwave test reactor from powdered iron ores (magnetite) with carbon as a reducing agent in a nitrogen atmospheric pressure environment [1]. The method has the potential advantage that the CO₂

emission can be reduced by tens of percent in conventional blast furnaces, if the electric power for the microwave is generated by renewable energy, such as solar, hydro and nuclear power [2]. A feature of the microwave method is the sudden rise in temperature of the material from ~700 °C to ~1000 °C accompanied by light emission of plasma, called the temperature jump [3]. The nature of the temperature jump is emergence of an additional energy flow to the material through the plasma.

The in-situ visible emission spectroscopy has been introduced to demonstrate the characteristics of the heating mechanism including volumetric and/or plasma surface heating [4]. The light emission after the temperature jump during the microwave ironmaking consists of strong atomic/molecular lines that can be assigned as those listed in the spectrum database based on the spark and arc discharge, indicating the presence of plasma electrons with several electron volts in the electron temperature. It was found that the structure of emission spectrum near-UV range (240 nm-310 nm) changes drastically from the continuous spectrum to discrete line spectra of iron with increasing surface temperature [3]. The continuous spectrum was assigned as a cathode luminescence due to the impingement of a plasma electron onto the sample surface of magnetite. It was also stated that the evolution from continuous spectrum to lines spectrum was the first observation to capture the progress of reduction process of iron oxide via in-situ spectroscopic method.

In those series of experiments, the multi-points spectroscopic and pyrometric measurements were

conducted. The purpose of this article, therefore, is to present the results obtained those multipoint systems. These results not only supplement the prior statement associated to the spectral evolution, but also demonstrate importance of the plasma surface heating in the reduction of iron ore after the temperature jump. Especially, the position dependency of the evolution of emission spectrum promotes deeper understanding of the plasma-surface interaction such as the reaction cycle being in the complex surface structure on the material.

2. Experimental setup

The multimode test furnace at the National Institute for Fusion Science is shown in Fig. 1. According to the concepts developed in Germany in order to improve the homogeneity of the electromagnetic field, the applicator shape is hexagonal [5]. The furnace is equipped with five magnetrons. The microwave power of one magnetron is 2.5 kW at a frequency of 2.455 ± 0.030 GHz. Two mode stirrers scatter the standing waves. Before starting the process, the chamber was evacuated by the rotary pump and refilled with nitrogen gas. During processing, a continuous nitrogen gas flow of about one liter/minute was used with a pressure a little higher than ambient pressure.

A multi-point emission spectroscopic diagnostic was conducted through the viewing port on the furnace. Ten sightlines with a distance of 2.2 mm and a spot diameter of 1.0 mm were provided by means of the fiber bundle and magnifying lens located above the furnace. Figure 2 shows the schematic of the sight lines for the spectroscopic measurement, as well as for the pyrometry. Seven sightlines, labeled as f1, f2... f7, are directed to the sample surface through the hole of the insulator board as the top-cover, and the remaining three (f8 - f10) are terminated by the surface of that insulator. The spectrometer was a Czerny-Turner imaging polychromator with a focal length of 250 mm. The exposure time was 2 s and the cycle time for capturing was 5 s [3].

InGaAs pyrometers (labeled as IR's in Figs.1 and 2) were taken for the temperature measurement. IR1, IR2, and IR3 were directed to the sample surface, the crucible outer surface and the crucible bottom, respectively. The detection wavelength range for IR1 and IR3 was $1.95 \mu\text{m} - 2.5 \mu\text{m}$, that for IR2 was $0.8 \mu\text{m} - 1.6 \mu\text{m}$. The spot size was 10 mm for IR1, 4 mm for IR2, and 3 mm for IR3. As shown in Fig.2, IR1 and f1 (mentioned before) were adjusted in such a way that they cross each other at the point at 15 mm above the bottom of the crucible along its central axis. It is noted that the position of the observation spot (i.e., intersection of the sight lines and surface of material) slides on the surface with increasing the surface temperature, since the powdered material shrinks and melts as shown schematically in Fig.2; the height of the powdered material

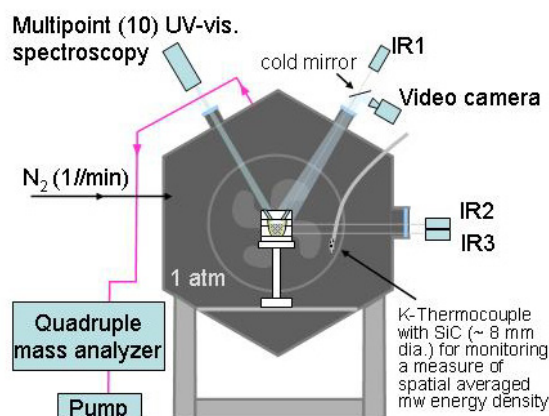


Fig.1 Schematic diagram of the multi-mode test furnace and diagnostics system. The opposite side distance of hexagonal cross-section is 1.1 m.

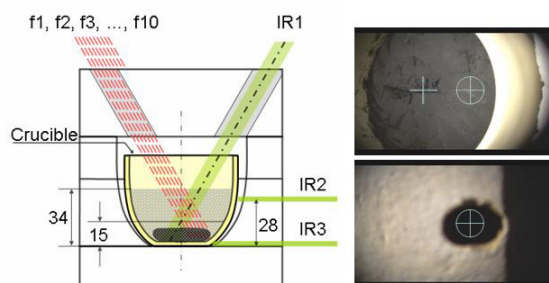


Fig.2 Sight lines for multipoint spectroscopic observation and configuration of material, crucible and insulator (left). Video camera pictures of the sample surface without top insulator (upper right) and with top insulator with the sight hole (lower right).

was set before the heating at 34 mm (light-shaded area), and this height changed to around 10 mm after the heating (dark-shaded area). The photograph at upper right in Fig.2 shows the surface of the material captured before heating by video camera located above the furnace (See also Fig.1). The central point of the cross-mark with circle of 10 mm in actual diameter indicates the sight axis of the IR1, and the left cross-mark is the observation spot of f1 for the initial height of the material.

The purified reagent of Fe_3O_4 with graphite was prepared according to the preparation performed in the prior experiment [3]. The mix ratio was $M_{\text{Fe}_3\text{O}_4} : M_{\text{C}} = 90 : 10$ ($= 54.0 \text{ g} : 6.0 \text{ g}$) by weight. Corresponding mol ratio was $n_{\text{Fe}_3\text{O}_4} : n_{\text{C}} = 1.0 : 2.0$. The crucible was thermally insulated by alumina-silica fiberboards as illustrated in Figs. 1 and 2.

3. Results and Discussion

3.1 Heating characteristics

Fig. 3(h) shows temperature traces obtained for IR1, IR2, and IR3. The heating mode is volumetric heating initially, but changes in plasma surface heating after the temperature jump at 740 s - 840 s. The series of the picture

at the lower of Fig. 3 depicts the surface condition captured by the video camera of which the field of view is indicated in Fig. 2. During the volumetric heating the bright crack structure on the surface as shown in the second picture labeled as $t = 185$ s continues, but the micro-scale discharge spark often occurs along the crack. After $t = 700$ s, the size of spark grows approximately each time it appears (see third picture labeled $t = 743$ s), and finally it triggers the large-scale emission like flame covering whole top surface (see fourth picture labeled $t = 840$ s). At the same time, the increase in temperatures by IR1 and IR2 becomes rapid, and the intense emission spectrum begins to be observed, which shows typical phenomena of the temperature jump. There is no jumping behavior in the temperature trace obtained by IR3, indicating the heating is mainly due to the plasma generated on the top surface of the material. In Fig.3(h) the dashed-dotted line by the label of SiC-TC, which means the temperature trace for the thermocouple tip covered with the silicon-carbide powder (see Fig. 1), represents the relative change in the measure of the spatial averaged microwave energy density. The temperature of the SiC-TC decreases at the temperature jump, implying the emergence of the plasma being the microwave absorber.

3.2 Evolution of the spectrum

Figures 3(a)–3(g) show the time evolution of the emission spectrum as a contour map for various position of the sight line of f1 - f7. It is found that the drastic transition from continuous spectrum to discrete spectrum is seen in every sight line. The temperature range for the transition is approximately 1050 °C -1250 °C that is consistent with that stated in prior report [3]. This range is coincident with the temperature range of high reduction rate for magnetite and wustite [1]; therefore, the decay of the continuous spectrum suggests the significant progress of the reduction process of magnetite.

Typical continuous and discrete spectrums appearing in the evolution are shown in Fig. 4. Almost all the discrete spectra are well assigned to the spectra of iron atom observed in arc and spark discharges, and the origin of the continuous spectrum has been considered to be cathodoluminescence of magnetite [3]. It should be noted that the spectral intensity of the continuous spectrum is at least three orders of magnitude larger than that of black body emission for present surface temperature around 1000 °C. The wavelength range of the continuous spectrum of the present results coincides with that of cathodoluminescence [6] and absorption spectrums [7] of magnetite. Therefore, the transition from continuous spectrum to discrete spectrum can represent the progress of reduction process from magnetite to iron.

From Figs. 3(a)–3(g), it is also noticed that the decay of the continuous spectrum begins earlier for larger number

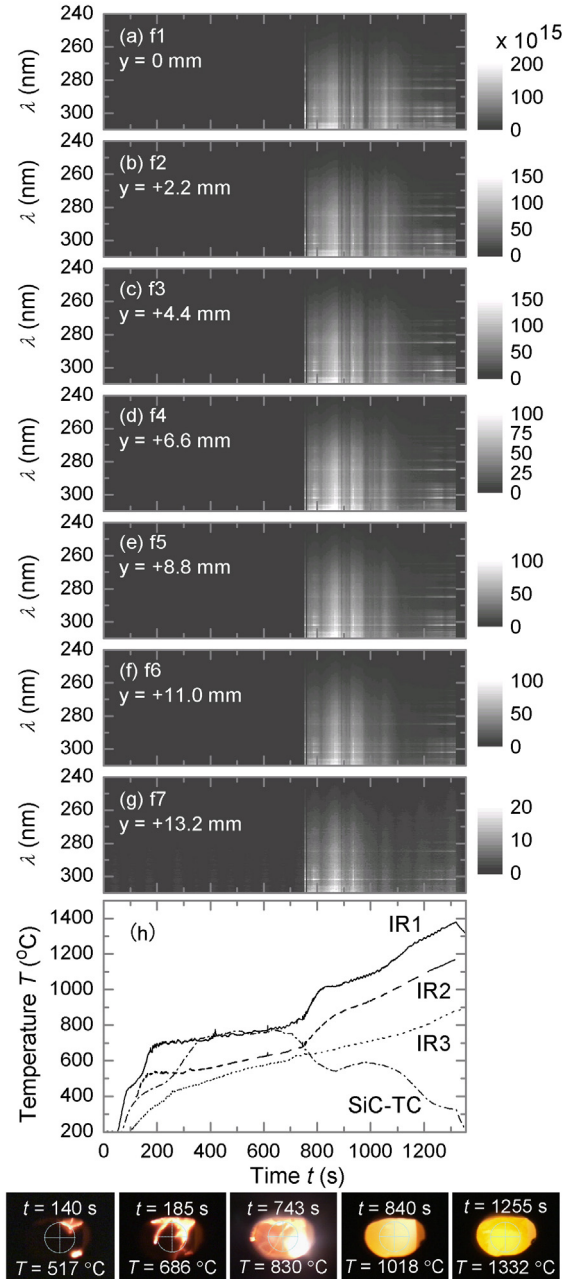


Fig.3 Time evolution of the emission spectrum for various sight lines (a)-(g). Temperature traces obtained for IR1, IR2, and IR3 (h). The temperature of SiC-TC (see text) is also included in (h). A series of the picture of the appearance of the surface (see also Fig.2).

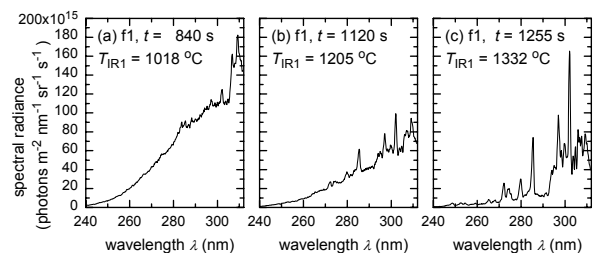


Fig.4 Emission spectrums appearing in the evolution. The peaks around 308 nm in (a) are OH spectrum. Almost all the peaks in (b) and (c) are spectra of iron neutral.

of the sight line. Figures 5(a) and 5(b) depict the time evolution of the spectral intensities, I_{SR} , at the wavelength of $\lambda = 289$ nm and $\lambda = 302$ nm. The former and latter wavelengths are associated to the continuous spectrum and the iron spectrum, respectively. In the intensity of the iron spectrum, the component of the continuous spectrum is already subtracted. It can be seen that the steady decrease in I_{SR} of the continuous spectrum ($\lambda = 289$ nm) is earlier for f5 than f1. The beginning time of the decreasing is $t \sim 950$ s for f5, but $t \sim 1050$ s for f1. On the other hand, the value of I_{SR} of iron spectrum ($\lambda = 302$ nm) for f1 increases moderately, but that of f5 decreases briefly at $t \sim 1100$ s, and then increases rapidly. These behaviors depending on the position vary smoothly spatially, which can be recognized by Fig. 5(c) for the continuous spectrum and by Fig. 5(d) for iron spectrum.

The possible interpretation for the position dependence is presented as follows. First, it is assumed that after the temperature jump the position of the observation spot for each sight line slides immediately for the edge of the material (toward the right hand side of Fig.2), because the material should shrink rapidly and its height drops substantially. This assumption has been based on the observation that the emission band spectrum of CN decays rapidly just after the temperature jump, implying the consumption of the space in the powdered material. Fundamental process on the surface is likely that when a part of the surface layer melts resulting from the reduction of iron oxide induced by the plasma bombardment, it clumps together and drops for the bottom. Then, in the central part of the material (near the axis of the crucible), the new surface layer of the powder material of iron oxide comes to the surface. The reaction cycle, such as reduction, clumping, and dropping, completes faster for nearer the edge of material, because the reaction cycle can also progress from the side surface of the material. This is reason why the continuous spectrum decays faster for nearer edge. The brief drop and the significant increases in the iron spectrum in the final stage of the heating can be related to the growth and decay of the large-scale crack structure that is found for the present case. The cracks grow via erosion with the reaction cycle, but they decay via melt meaning the end-state of the reaction. In present case the brief drop can be due to escaping of material from the observation spot with growing the crack, and significant increase can be due to returning of the material to the observation spot with spreading the melt region.

4. Summary

We presented the experimental results obtained by the multipoint spectroscopic and pyrometric measurements during the microwave ironmaking. Both results demonstrate the importance of the plasma surface heating in the reduction of iron ore after the temperature jump.

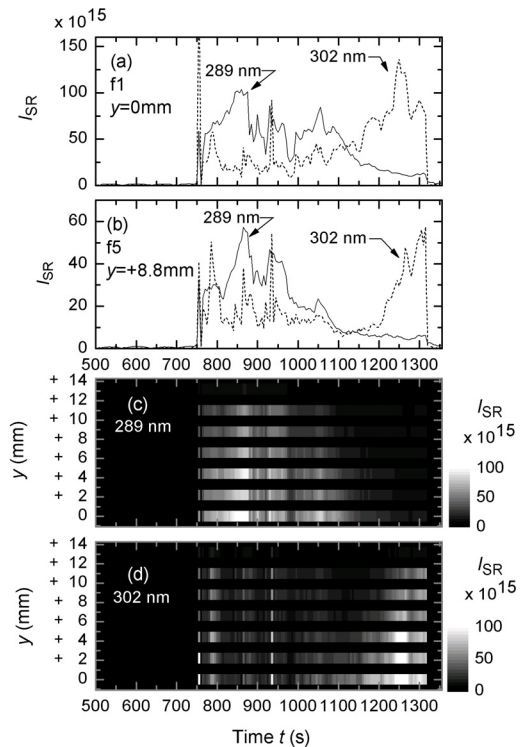


Fig.5 The time evolution of the spectral intensity, I_{SR} , (spectral radiance in the unit [$\text{photons m}^{-2} \text{s}^{-1} \text{sr}^{-1} \text{nm}^{-1}$]) at the wavelength of $\lambda = 289$ nm and $\lambda = 302$ nm for the sight line of f1 ($y = 0$ mm) in (a) and f5 ($y = 8.8$ mm) in (b), and for various position of the sight line as the contour map in (c) for $\lambda = 289$ nm and (d) for $\lambda = 302$ nm, respectively.

Especially, the position dependencies of the evolution of continuous spectrum and iron spectrum make us address the reaction cycle on the large-scale surface structure in the material.

Acknowledgement

This research is supported in part by a Grant-in-Aid for Scientific Research on Priority Areas (465) of the Ministry of Education, Culture, Sports, Science and Technology in Japan.

References

- [1] K. Ishizaki, et al., *ISIJ*, **46**, 1403 (2006).
- [2] K. Nagata, et al., *Proc.11th International Conference on Microwave and High Frequency Heating*, (3-6 Sep 2007, Oradea, Romania) pp. 87-90.
- [3] A. Matsubara, et al., submitted to *JMPEE*.
- [4] M. Sato, et al., *Proc.10th International Conference on Microwave and High Frequency Heating*, (11-15 Sep 2005, Modena, Italy) p.p. 272-275.
- [5] L. Feher, et al., DE-PS 19633245C1 (27.11.1997);
L. Feher, et al., DE-PS 10329411 (31.1.2005).
- [6] I. Balberg, et al., *Phys. Rev. Lett.* **27**, 1371 (1971).
- [7] P.A. Milies, et al., *Rev. Mod. Phys.* **29**, 279 (1957).